Shear-induced mechanochromism in polydiacetylene monolayers

A.R. Burns [a,*], R.W. Carpick [a,**], D.Y. Sasaki [a], J.A. Shelnutt [a,***] and R. Haddad [b]

[a] *Sandia National Laboratories, MS 1413, Albuquerque, NM 87185-1413, USA*
E-mail: aburns@sandia.gov
[b] *Department of Chemical Engineering, University of New Mexico, Albuquerque, NM 87131, USA*

We use atomic force microscopy to actuate and characterize the nanoscale "mechanochromism" of polydiacetylene monolayers on atomically-flat silicon oxide substrates. We find explicit evidence that the irreversible blue-to-red transformation is caused by shear forces exerted normal to the polydiacetylene polymer backbone. The anisotropic probe-induced transformation is characterized by a significant change in the tilt orientation of the side chains with respect to the surface normal. We discuss preliminary molecular dynamics simulations and electronic structure calculations on twelve-unit polydiacetylene oligomers that allow us to correlate the transformation with bond-angle changes in the conjugated polymer backbone.

KEY WORDS: atomic force microscopy; friction force microscopy; friction anisotropy; shear force microscopy; nanotribology; polydiacetylenes; LB films; molecular mechanics; conjugated polymers

1. Introduction

As evidenced by other articles in this issue, organic films of ordered, densely-packed molecules have been used extensively as model lubricants to study the structural, mechanical, and chemical aspects of adhesion and tribology. In most cases, these films are monolayers of simple alkanes, of variable chain length and tail group chemistry, that are created either by Langmuir–Blodgett (LB) [1] or self-assembly techniques [1,2]. We have been working on another class of organic thin films that are also composed of densely-packed alkane chains; each chain, however, has an integral diacetylene unit (figure 1(A)). The distinguishing feature of these films is that the molecules may be cross-linked via UV photochemistry in a one-dimensional fashion to form highly-ordered arrays of long polydiacetylene (PDA) polymers (figure 1 (B) and (C)). These films have been the subject of many years of research [3] because the cross-linking produces a conjugated backbone that exhibits a chromatic response to elevated temperature, solvents, and stress. Mechanically-induced color changes, or "mechanochromism" [4], offers an intriguing potential use in tribology as an optical sensor of contact, friction, and adhesion. Thus our motivation in this paper, and that of a previous study of PDA trilayers [5], is to understand what molecular changes (e.g., disordering, re-orientation) are involved in the friction-induced mechanochromism of PDA monolayers. To accomplish this, we use scanning probe microscopy to both actuate and characterize the structural changes of the PDA films. Since these are unusual films, we will first discuss some of their salient features.

In figure 1, we show the basic structure of a PDA monolayer that is created on a LB trough and transferred to a solid substrate. An ordered monomer phase (B) is formed and then polymerized (C) with UV light. The linear conjugated backbone is parallel to the LB subphase and retains this geometry when transferred to the substrate surface (D). Thus it is bound to the substrate via an interaction with the (hydroxyl) head groups on the lower set of side chains, while the upper set of side chains and methyl tail groups becomes the "interface" with probe tips, analytes, solvents, etc. Using optical and atomic force microscopy (AFM), we have shown that the polymer backbones align in highly parallel arrays in domains exceeding 100 μm^2 [5–7]. The lengths of

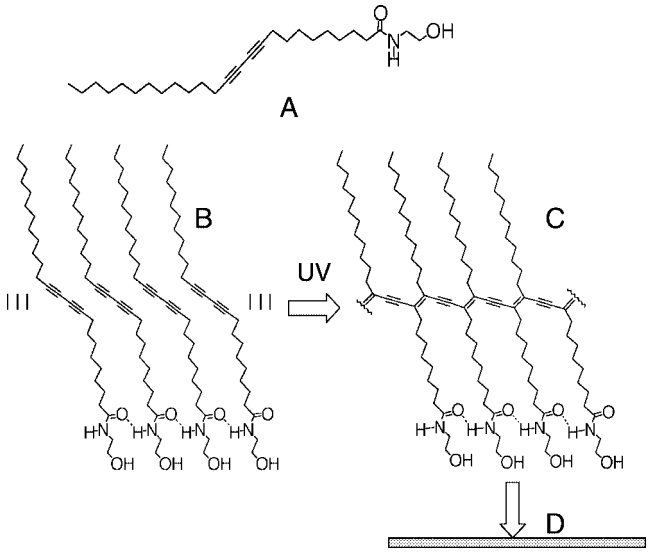

Figure 1. (A) Diacetylene monomer N-(2-ethanol)-10,12-pentacosadinamide. (B) Ordering of monomers under 20 mN/m pressure on LB trough, followed by UV polymerization into (C) polydiacetylene (PDA). (D) The PDA monolayer is horizontally transferred (head groups down) to a hydrophilic SiO_2 substrate.

* To whom correspondence should be addressed.
** Current address: Department of Engineering Physics, University of Wisconsin-Madison, 1500 Engineering Dr., Madison, WI 53706-1687, USA.
*** Current address: Department of Chemistry, University of New Mexico, Albuquerque, NM 87131, USA.

1023-8883/01/0300-0089$19.50/0

the side chains and the chemistry of the head and tail groups can be modified much in the same manner as for the model lubricant alkanethiols or silanes [7–11]. In this paper, we use a hydrophilic silicon oxide substrate because, like mica, it is atomically flat and interacts with the transferred film via hydrogen bonding. Unlike metallic substrates, the thick thermally-grown oxide layer (80 nm) of the silicon substrate prevents quenching of the optical excitations. The weaker hydrogen-bonding, relative to the strong covalent bonding of thiol linkages to gold [11], allows for greater molecular motion about the backbone (discussed below), yet is sufficient for robust, good quality films. Mica offers the same qualities as the silicon oxide, along with possible ionic bonding to K^+ impurities.

The intense optical absorption characteristic of PDA, and of conjugated polymers in general [12–14], is caused by the excitation of π electrons in the extended linear backbone. Both absorption and fluorescence (if any) in the visible region tend to be highly polarized along the backbone direction. We have shown that the large domains of crystalline alignment exhibit strong polarization extinction [5,7,15]. The blue-shift in the absorption spectra which characterizes the thermally-, chemically-, or stress-induced chromatic transition of PDA from the "blue" form to the "red" form is shown in figure 2. A very important feature of these PDA films is that the red form exhibits intense fluorescence (see dotted curve in figure 2), whereas the blue form does not. *Thus we are able to use fluorescence as an optical signature of the mechanochromism, thermochromism [6], etc*. The fluorescence can be detected simultaneously by using a near field scanning optical microscope (NSOM) [5] or verified subsequent to AFM actuation with a conventional optical microscope. The NSOM is ideally the best tool because it can actuate and detect the fluorescence; however, AFM offers far superior topographical lateral and height resolution. Since the latter is more critical for determining the structural changes associated with the PDA mechanochromism we have taken that approach in this article.

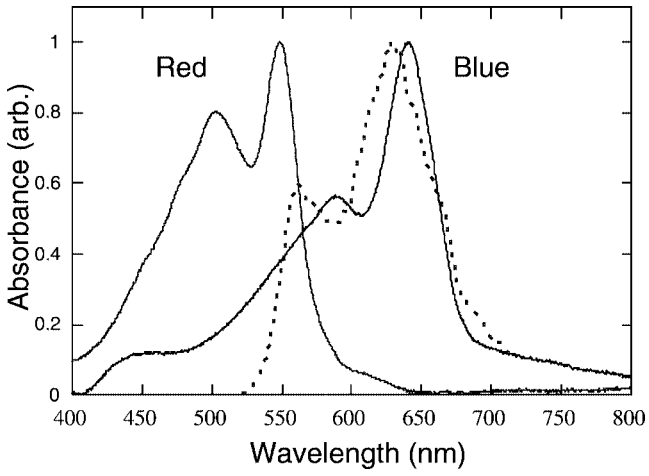

Figure 2. Visible absorption spectra of "blue" and "red" form PDA trilayer films; (- - -) is the fluorescence spectrum of the red form. The blue form does not fluoresce.

The blue-shift of the absorption in going from the blue to the red form is not fully understood, but is generally associated with "strain" imposed onto the conjugated backbone by the side chains [16]. As depicted in the highly schematic figure 3, the blue form is thought to be in the planar all-*trans* geometry, where the side chains are in the same plane as the backbone. This geometry permits extended, continuous π overlap or "conjugation length" [17–20]. Out-of-plane conformations in the side chains disrupt the π overlap which shortens the conjugation length and blue-shifts the absorption spectrum to that of the red form (figure 3). Note that out-of-plane rotation of the side chains requires possible rupture and reformation of the surface bond; thus strong covalent bonding to the substrate may hinder this rotation. The exact correlation between the conformational geometry and the electronic structure is not known. We address this problem by using a molecular dynamics (MD) simulation followed by electronic structure calculations. In this preliminary effort, we use twelve repeating unit energy-minimized oligomers of PDA on which we perform the MD. The resulting conformational changes in the backbone, particularly dihedral angles induced by side chain movement, are then correlated with the calculated electronic structure and absorption spectra. In this way, we are able to estimate minimum conformational changes for color shifts.

In our earlier study of mechanochromism in PDA [5], we presented results consistent with the notion of side chain rotation out of the backbone plane. However, that study was restricted to *trilayers*, since LB monolayers of the 10,12-pentacosadiynoic acid monomer precursor are not stable on a pure water subphase. We found that the shear-induced blue-to-red transformations were complicated by the removal of the top bilayer, revealing a seemingly "flattened" monolayer underneath. Thus molecular-scale aspects of conformation changes in the transformation were obscured by the trilayer geometry. It became clear that stable *monolayer* films were required to simplify characterization of the transformation. Since then, we have been able to produce stable monolayers by synthesizing the monomer N-(2-ethanol)-10,12-pentacosadinamide [7] (figure 1(A)). The monolayer stability is due to inter-chain H-bonding at

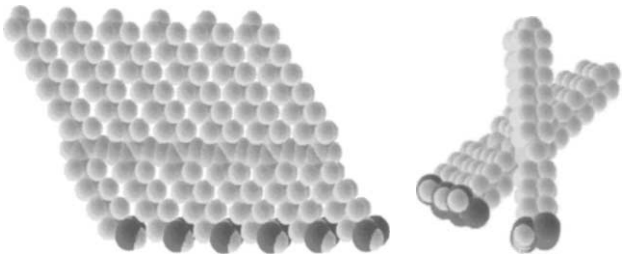

Figure 3. Highly schematic model for the blue and red PDA forms. The planar "blue" form at left has unbroken π-electron overlap and a full conjugation length. At right, the out-of-plane side chain rotation has broken the π-electron overlap in the "red" form, reducing the conjugation length.

the head groups. In this report, we thus describe evidence of side chain rotation actuated by AFM probe tips.

2. Methods

2.1. Sample preparation

Si substrates with 80 nm thick thermally-grown oxide were cleaned in organic solvents followed by a 50/50 mixture of 30% H_2O_2 and concentrated H_2SO_4 for 20 min at 100 °C, then immediately rinsed and stored in pure water before transfer to the LB trough. AFM images indicated very little observable contamination and verified that the substrates were extremely flat, with <2 Å RMS roughness. Just prior to monolayer spreading, the substrates were removed from water storage and completely immersed into the trough subphase, minimizing exposure to air. The Si substrate was seated horizontally approximately 1 mm below the subphase surface.

PDA monolayers were prepared via UV polymerization on the LB trough that rests on a vibration isolation table inside a class 100 clean room. The pure water subphase had a resistivity greater than 18 MΩ cm and was held at a temperature of 15 ± 1 °C. The monomer N-(2-ethanol)-10,12-pentacosadinamide (structure (A) in figure 1) was synthesized as described elsewhere [7] and dissolved in 50% chloroform/benzene for dropwise spreading on the subphase. All films were equilibrated for 20 min at 20 mN/m, prior to UV light exposure from a pair of Hg pen lamps whose output is dominated by the 254 and 365 nm lines. To produce a uniform blue film, the pen lamps were fixed 15 cm from the compressed monolayer (23 μW/cm^2) and switched on for 30 s. Horizontal transfer of the blue films was accomplished by slowly lowering the polymerized film onto the parallel Si substrate by draining the trough. Samples were dried in clean room air and stored in a dark, nitrogen-purged container. More details may be found in [7].

2.2. Atomic force microscopy, fluorescence microscopy

The AFM (Multimode Nanoscope IIIA, Digital Instruments) was operated in contact mode under ambient conditions with a single silicon nitride cantilever and tip. We used the nominal force constant of 0.06 N/m for the calculated loads. More scanning details are discussed in section 3.1. To verify that the PDA blue form was converted into the fluorescent red form, samples were removed from the AFM and placed under a Leitz fluorescence microscope that used 520–550 nm excitation and a 590 nm long-pass filter. An example of this method is shown in figure 4.

2.3. Molecular dynamics and quantum calculations

The molecular mechanics (MM) and molecular dynamics (MD) simulations were performed with PolyGraf software (Version 3.21) using a Dreiding II force field for atomic interactions. The dielectric constant was set to 2.64, and charges were assigned using the charge equilibration method. A canonical MD simulation using the Hoover formalism was then setup for a total run time of 500 ps with the temperature set at 300 K. Following the MM and MD calculations, the electronic properties of the conjugated backbone in its various configurations at selected intervals (e.g., 80, 100, and 128 ps) were calculated using ZINDO/S semiempirical methods on the HyperChem 5.02 software package.

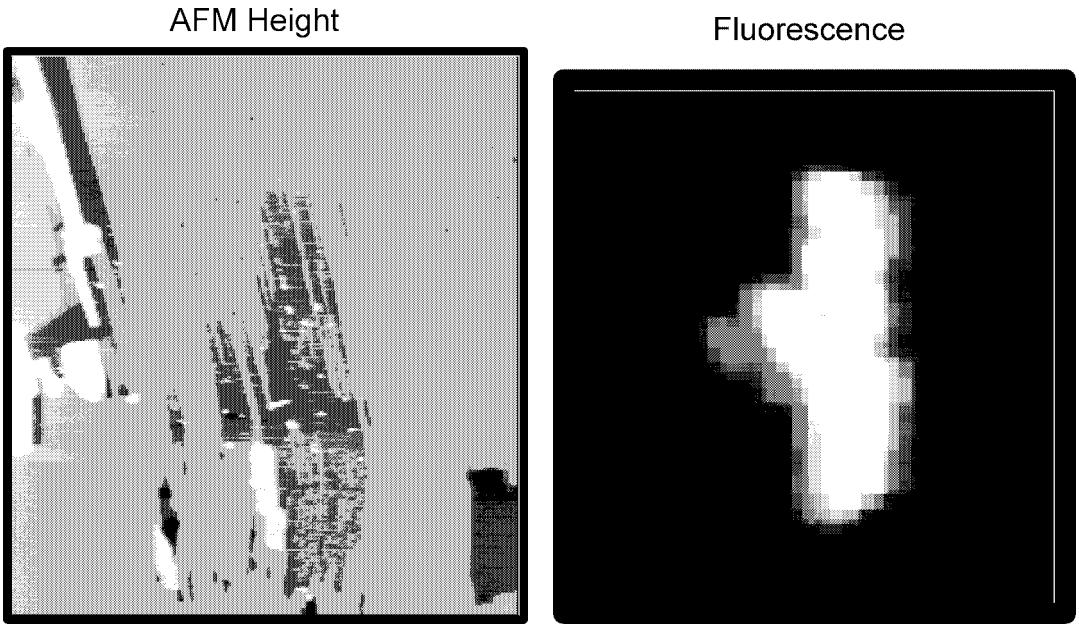

Figure 4. Left side, 10 × 10 μm^2 topographic AFM image showing tip-induced conversion of the blue form into the fluorescent red form of PDA. Note that the red region appears lower than the surrounding blue region. Right side, fluorescence microscope image of same region. From [5].

3. Results

3.1. AFM-induced mechanochromism of PDA monolayer

In this section, we present AFM images that are representative of the mechanically-induced blue-to-red transformation of the PDA monolayer. They provide us with fairly detailed structural information concerning the transformed regions, how they differ from the initial blue regions, and insight into how the "mechanochromism" takes place. In all cases, the transformation is irreversible, even after several weeks. Other than the transformation, we saw no evidence for monolayer instability or AFM-induced damage to the films.

We show in figure 5 the 1×1 μm^2 height and friction AFM images of an initially blue PDA monolayer (near a bare silicon oxide defect) that was in the process of being transformed into a red region. The transformation only occurred with sliding contact between the tip and sample, and took place during repeated scanning (>30 scans) at an estimated load of 6 nN and scan rate of 4.5 Hz. Imaging at very low loads (0 to -20 nN) and a 3 Hz rate, in the absence of significant adhesion, allows us to image the sample without inducing further transformation. The rate of growth of the red areas proceeds faster at larger loads; however, variation from sample to sample and even within one sample makes it difficult to quantify the exact load dependence of the transformation rate.

The transformed (red) regions, particularly in the friction image, reveal the backbone direction (indicated by the arrows) via striations that may be due to uneven packing density of the individual backbones [15]. Note that the scan direction is almost normal to the backbone direction in the upper region, which appears to have transformed to a greater extent (probably faster) than the lower region of the image. In most cases, the transformation proceeds most rapidly when the sliding (fast scan) direction is perpendicular to the backbone direction. Usually, it will not proceed at all when the fast scan direction is parallel to the backbone direction. Thus, *shear forces are required*. These observations are consistent with the shear-force anisotropy that was observed to be a function of chain orientation (highest forces being perpendicular to chain direction) for PDA monolayers on mica [15] and gold [21]. We note a factor of three in the ratio between high and low friction forces (for sliding perpendicular and parallel to the backbones, respectively). Unfortunately, our cantilever in the present work was not calibrated for quantitative shear force measurement. However, we do not expect the shear forces to differ appreciably from the AFM results reported by Mowery et al. [21], for PDA monolayers on gold, where the anisotropic shear forces were in the range 10–35 nN for loads below 20 nN.

Defects in the blue film such as the bare SiO_2 area assist significantly in the initial formation and growth of the red domains. The red regions appear to nucleate at the edge of the hole. In general, we find the growth of the red domains is strongly anisotropic, with preferential growth along the backbone direction. Furthermore, we find that the transformation may propagate along the backbone direction *beyond* the region where shear stress has been applied.

From the molecular modeling calculations (below) we estimate that the head-to-tail distance of the all-*trans* PDA (figure 1) is approximately 31.7 Å. AFM measurements under light imaging loads (0 to -20 nN) determined a blue-form PDA film thickness of 27 ± 3 Å. Thus the nominal molecular tilt angle of the blue film is $30° \pm 10°$, which is consistent with previously reported values of multilayer films [22,23]. The blue regions in figure 6 are 22 ± 2 Å thick ($45° \pm 5°$ nominal tilt) and the transformed red regions are 9 ± 0.9 Å

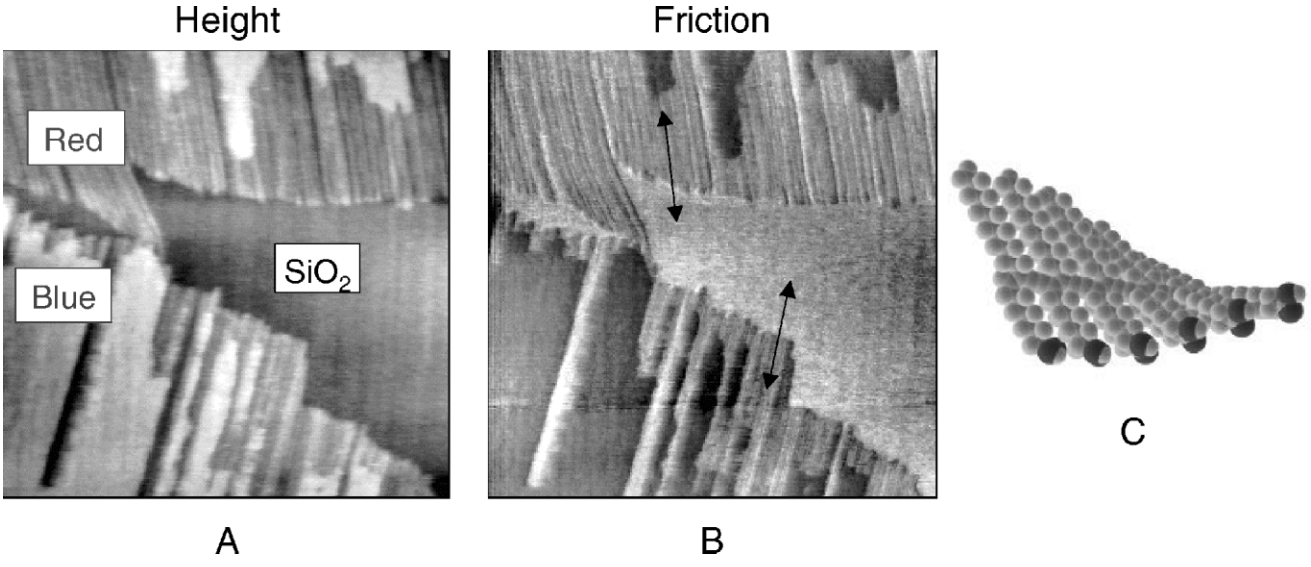

Figure 5. Height (A) and friction (B) images (1×1 μm^2) of region that was transformed under AFM shear forces. Arrows indicate backbone directions. The fast scan direction is along the x-axis. The original blue (brightest in (A), darkest in (B)) and transformed red regions are labeled as well as the bare substrate (darkest in (A), brightest in (B)). The heights of the blue and red areas relative to the substrate are 22 ± 2 and 9 ± 0.9 Å, respectively. (C) Schematic representation of blue-to-red transformation.

thick (74° ± 2° nominal tilt). *Thus it appears that the side chains are being pushed towards the substrate by the tip as it scans perpendicular to the backbone direction.* We depict this schematically in figure 6(C). It is important to note that the morphology of the mechanically-transformed red region appears to be different from the closely-packed, upright morphology of thermally-transformed red multilayer films [22] or photochromic red monolayers made on the LB trough with excessive UV exposure [7,15]. However, all three red forms have identical fluorescence spectra and comparable emission intensities. This leads us to conclude that neither the overall polymer orientation with respect to the substrate nor the packing density significantly influence the optical properties of the red films. Instead, we believe that it is the local strain on the backbone by the (re-oriented) side chains that is the important aspect.

The friction in the red transformed regions increases up to 100% relative to the blue regions. Moreover, the lowest red PDA regions have the highest friction. Thus the friction appears to correlate directly with the compression or re-orientation of the side chains towards the surface. Much of the friction in the transformed regions is most likely due to increased disorder of both the side chains and the backbone packing. However, the re-orientation will also expose the side chain methylene (–CH_2–) groups and the conjugated backbone. Since these have a higher surface energy than the methyl (CH_3) tail groups [24], it is likely that a component of the higher friction is due to an increased adhesive interaction with the tip.

Since the AFM tip causes a re-orientation of the PDA side chains in the manner described above, more steric freedom is needed to accommodate the increased area per molecule. This is a primary reason why the transformation is facilitated near bare spots and defects. This can be seen in figure 6, where the backbone direction is parallel to the edge of the hole and almost perpendicular to the scan direction. Both aspects readily facilitated the conversion; we see growth of the red area along the backbone direction and perpendicular to it. The 1×1 μm^2 height and friction images were acquired *during* the transformation, thus they are "stills" from

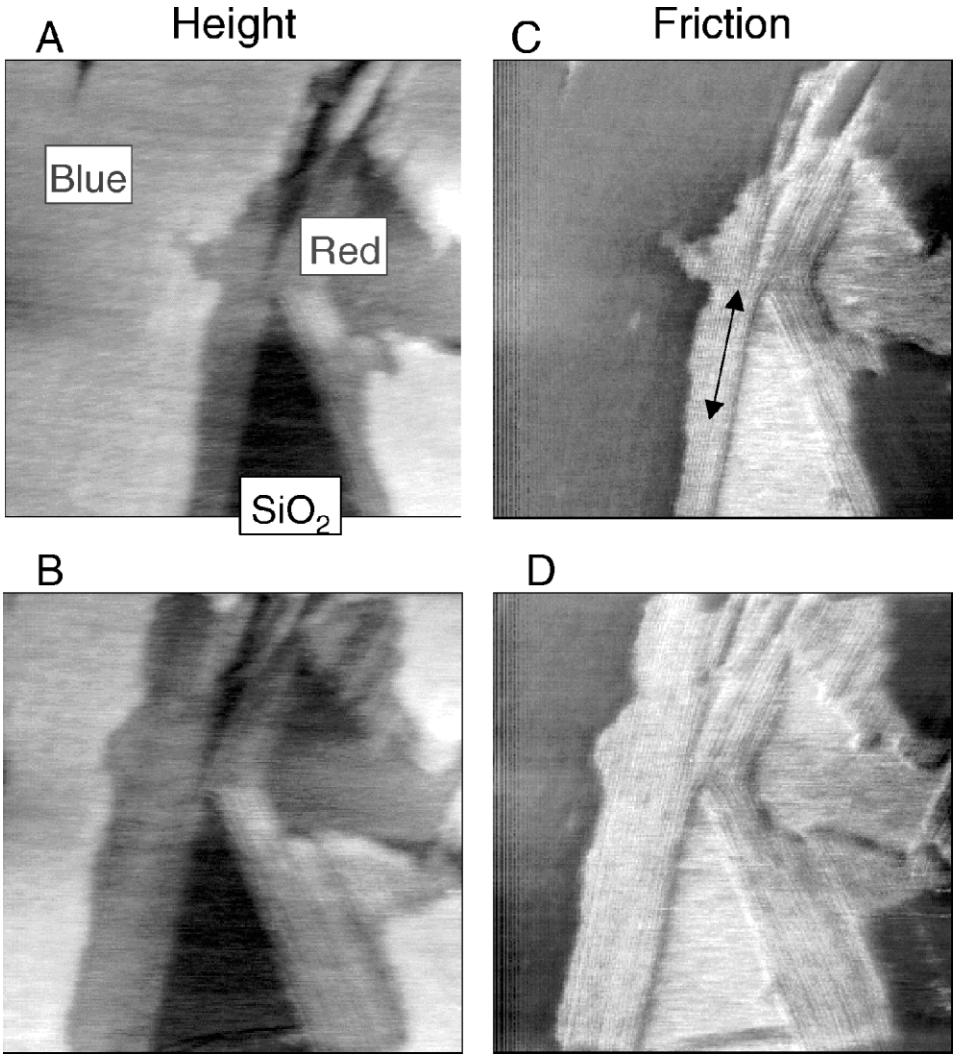

Figure 6. Consecutive height and friction images (1×1 μm^2) acquired *during* blue-to-red transformation by AFM shear forces. (C) and (D) were acquired 28 frames after (A) and (B) at scan rate of 4.5 Hz. The arrow indicates backbone direction and the blue, red and substrate areas are marked. See text for details.

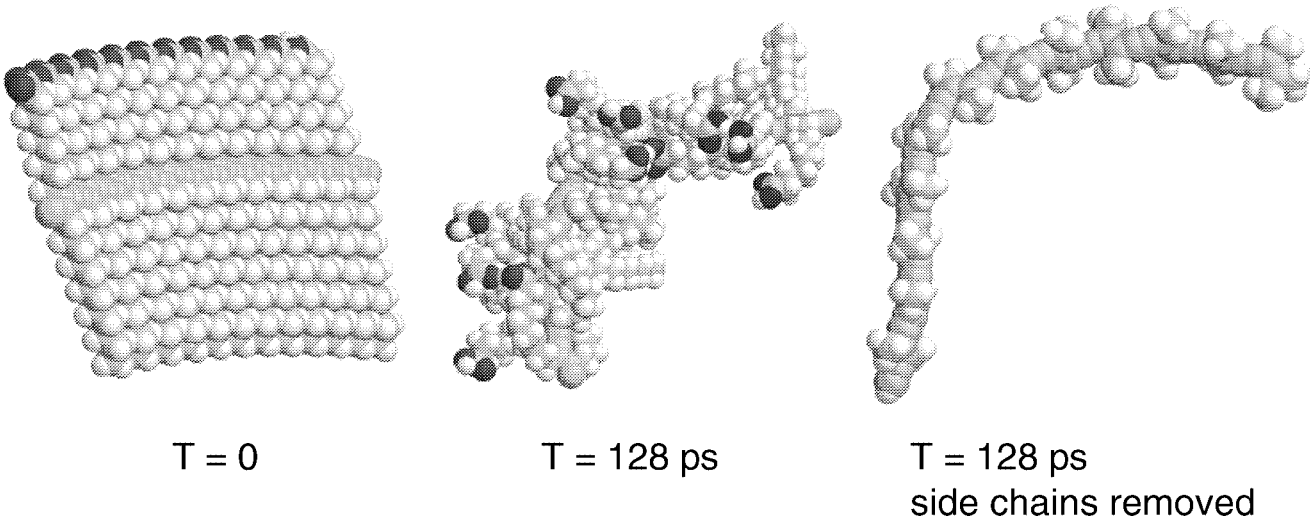

Figure 7. Left part, twelve-unit planar PDA oligomer ("blue" form) minimized by molecular mechanics (note head groups are on top) prior to MD simulation. Middle part, same oligomer after 128 ps of the MD simulation. Right part, same 128 ps structure with side chains "pruned" for quantum calculations. The clipping takes place *after* the simulation and is used to simply the quantum calculations.

a long sequence of images: (A) and (C) under a 6 nN load and scan rate of 4.5 Hz, while (B) and (D) were acquired 28 frames later under an increased load of 17 nN. The transformation rate was observed to increase with higher load, but eventually decreased (at the same higher load) as the red region progressed farther from the bare substrate. Thus the side chains were now sterically hindered from re-orienting at the same rate. Once again, the friction contrast is substantial between the red and blue regions.

3.2. Molecular mechanics and electronic structure calculations

The results presented above clearly indicate that the shear forces experienced by AFM tip are due to an interaction with the side chains that alters their orientation with respect to the original plane of the all-*trans* "blue" form. Out-of-plane rotations of the side chains will disrupt the π-orbital overlap or "conjugation length," causing a blue shift of the absorption. One of the primary motivations in using the PDA monolayers is the potential use of its mechanochromism as an optical transducer of disordering, film defects, or shear forces. In this section, we briefly discuss our initial efforts to use MD and electronic structure calculations to determine quantitatively what the minimum angle changes are that result in the absorption shifts.

Two oligomers with differing headgroups were examined in the MD simulations. The first one was terminated with the carboxyl head groups of 10,12-pentacosadiynoic acid, while the other was terminated with the amide head groups of N-(2-ethanol)-10,12-pentacosadinamide (shown in figure 1(A)). The latter is expected to exhibit hydrogen bonding between head groups. Each all-*trans* PDA oligomer was made twelve units long (i.e., twelve sets of side-chains above and below the backbone), and minimized by molecular mechanics where it remained planar and ordered. This is shown at left in figure 7. During the 500 ps time scale of the 300 K MD simulation, the side chains of the oligomers became highly disordered and the backbones developed bends due to out-plane side chain rotations (see middle of figure 7). These thermal fluctuations of the isolated oligomers are expected, whereas in a close-packed film, the polymers would be more stabilized by their neighbors. However, for the present purposes, the fluctuations allow us to quantitatively sample backbone geometries and corresponding electronic structures for various conformations.

Structural analysis was performed on the molecular geometries at fixed intervals (<0.25 ps) during the 500 ps simulation. For the structure at each time interval, eleven dihedral angles (between the twelve units in the chain) were calculated along the backbone. The dihedral angles were measured from one C=C double bond to the next, as shown below:

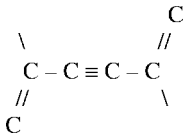

In the dihedral angles reported, the origin (0°) is set at what is traditionally defined as 180° since this is the starting (planar) configuration. This convention makes it easier to look at the deviations from planarity. The "average dihedral angle" is used as an index of overall deviation from planarity in the oligomer. The sign of the angles is unimportant, hence the average uses the absolute value.

In figure 8, we show the average dihedral angle vs. MD simulation time for the two oligomers with differing head groups. In both oligomers we see significant deviations from planarity early on in the simulation. The upper curve (A) is for the oligomer made from 10,12-pentacosadiynoic acid, which does not make stable PDA monolayers. The lower curve (B) is for the oligomer based on N-(2-ethanol)-10,12-pentacosadinamide, that does make stable PDA monolay-

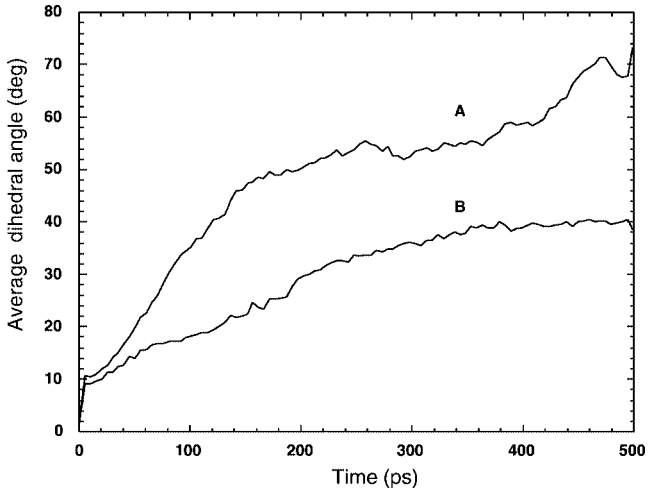

Figure 8. Calculated average dihedral angles vs. time from the molecular mechanics and dynamics simulation at 300 K. Curve (A) is for the twelve-unit oligomer with the COOH head group, and curve (B) is for the amide head group shown in figure 1(A) (see text).

ers. We see evidence of hydrogen bonding between the amide head groups in the smaller average dihedral angles at each time interval relative to the simulation for COOH head groups. Thus the hydrogen bonding not only stabilizes the monolayer on the LB trough, but it also tends to counteract out-of-plane side chain rotation.

After the MD simulation, some geometries (e.g., at 0, 80 and 200 ps), were selected for the quantum calculations on the conjugated backbone. To considerably shorten the time required for these calculations, all side groups were "clipped" off, leaving methyl groups in their place. Hydrogens added to the methyl carbons were minimized using molecular mechanics while holding the backbone and methyl carbon positions fixed. A bent and clipped oligomer is shown at right in figure 7. In figure 9, we show the calculated absorption spectra of oligomers selected from curve (A) of figure 8. (Once the oligomers are clipped it makes no difference which molecule was used for the quantum calculations. Curve (A) offers a bigger range of dihedral angles than curve (B).) For visualization purposes, the absorption spectra are generated from summing Lorentzian curves of oscillator strengths about the highest-occupied to lowest-unoccupied singlet transitions. Hence, the line shapes and widths are arbitrary. We also make no assignments concerning symmetry, so many of the transitions may be weakly allowed. Regardless, the important information presented here is the *blue-shift* in the spectra due the change in backbone π-orbital energies during the molecular dynamics simulation. One can see in figure 9 that there is a definite blue-shift with increasing average dihedral angle (values taken from curve (A) of figure 8). We also see that there is a rapid shift from $t = 0$ to 80 ps, followed by relatively no change after 200 ps. It is important to note that these spectra are instantaneous "snap shots" rather than averages, thus there can be large fluctuations in line position with time (e.g., see spectra at 200 ps).

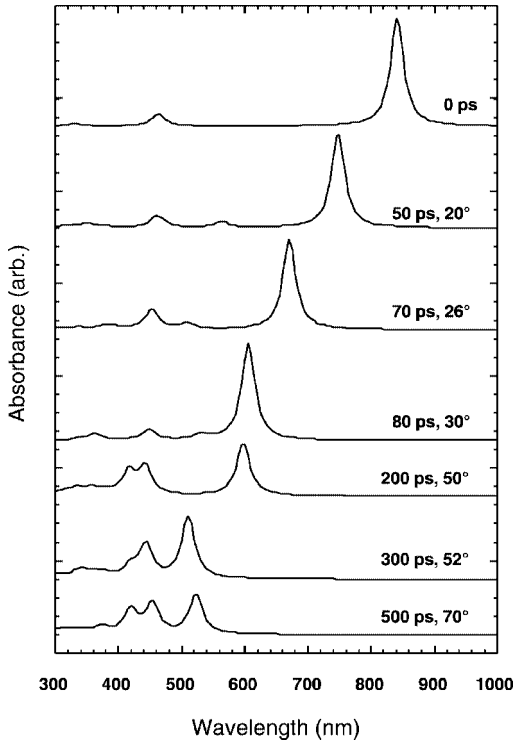

Figure 9. Absorption spectra from the quantum calculations for clipped oligomers at various times during the MD simulation. The arbitrary Lorentzian line shapes and widths are for visual purposes only. Also shown is the average dihedral angle from curve (A) of figure 8 for the oligomer at the specified time.

The blue-shifts in the spectra are caused by dihedral rotations of the side chains that break the π-orbital overlap and shorten the conjugation length. Two important questions arise: What critical angle is required to break conjugation in a way that shifts the absorption spectrum? What is the maximum conjugation length during the simulation for that critical angle? We try to answer these questions by using the index "conjugation length," which for a certain critical angle γ, we define as the longest backbone length (within the whole twelve-unit oligomer) that is not "broken" by an angle greater (absolute value) than γ. The results are shown in figure 10 for a few selected γ. We see that for $t < 5$ ps in the MD simulation there are some $<5°$ dihedral rotations. The conjugation (backbone) length between these $<5°$ rotations drops from the initial twelve units to four, followed by a gradual change to two units over the next 200 ps. However, if we compare this index to the spectral shifts in figure 9, we see that those shifts clearly have a different time dependence and must have required $\gamma \gg 5°$. *Thus we can rule out very small dihedral angles from our analysis.* In contrast, for $\gamma < 80°$, there is essentially no change in the conjugation length before 50 ps, yet we see significant spectral shifts in figure 9 before 50 ps. Thus we conclude that the conjugation is broken for dihedral angles smaller than 80°. (γ greater than 90° will tend to "re-form" conjugation as they approach 180°, and perhaps theoretically should not be counted as "breaking" the conjugation. In our computations, however, this effect was neglected since our dynamics

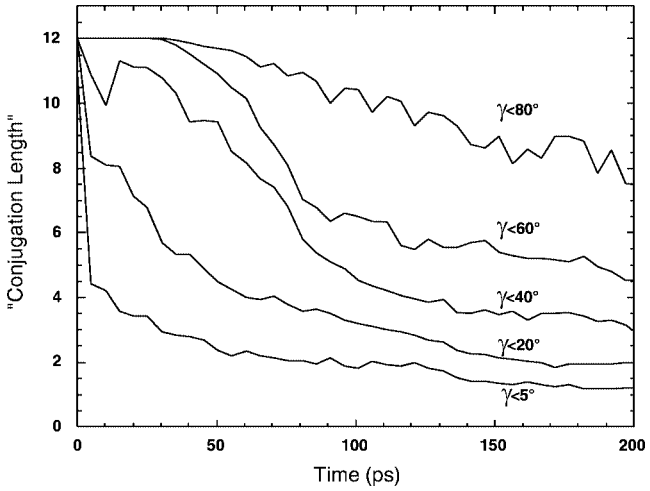

Figure 10. "Conjugation length" of oligomer vs. time during the MD simulation. The length, which for a certain critical angle γ, measures the longest backbone length (within the whole twelve-unit oligomer) present that is not "broken" by an angle greater (absolute value) than γ.

simulation did not go on for long enough for it to become significant.) For $20^\circ < \gamma < 60^\circ$, the analysis becomes some less obvious. If we assume that the shift is roughly linear from 0 to 80 ps, and rapidly levels off after $t = 80$ ps, then the "best fits" appear for critical angles γ in the range 40°–60°, and that the conjugation length for the "red form" is less than six units.

We conclude this section by noting that we can use the above analysis as a rough guide to morphological *changes* are required to observe mechanochromism. For the isolated twelve-unit oligomer, those average changes are 40°–60° side chain rotations at least once every six units. Clearly, a more detailed analysis is required, including longer oligomers, nearest-neighbor interactions, and substrate effects. However, we can conclude that very *small* changes in the blue form morphology are insufficient for mechanochromism, which is consistent with the AFM results discussed above, and consistent with the 18 kcal/mol activation energy required for trilayer thermochromism [6].

4. Conclusions

We have used AFM to actuate and characterize the "mechanochromism" of PDA monolayers on silicon oxide substrates. The blue-to-red transformation was analyzed in detail and found to be dependent on the shear forces exerted on the pendant side chains. Those shear forces perpendicular to the backbone direction were most effective in the transformation, which was also facilitated by defects and neighboring areas of bare substrate. Overall, the transformation was the result of significant side chain rotation towards the substrate. We presented preliminary modeling results on isolated twelve-chain oligomers that will help us correlate the molecular structure changes such as side chain rotation with the color changes of the PDA films. So far, we find that dihedral angle deviations from the blue planar form must be in the range of 40°–60°, every six units, in order to see shifts in the absorption spectra that compare with those observed experimentally. The irreversible nature of the chromatic conversion is somewhat limiting in its potential use as an *in situ* optical sensor. However, recent successes in reversibility in modified PDA vesicles [10] may lead to much more versatile and functional organic thin films.

Acknowledgement

RWC acknowledges the support of the Natural Sciences and Engineering Research Council of Canada. Sandia is a multiprogram laboratory operated by Sandia Corporation, a Lockheed Martin Company, for the United States Department of Energy under Contract DE-AC04-94AL85000.

References

[1] A. Ulman, *Introduction to Ultrathin Organic Films from Langmuir–Blodgett to Self-Assembly* (Academic Press, New York, 1991).
[2] L.H. Dubois and R.G. Nuzzo, Annu. Rev. Phys. Chem. 43 (1992) 437.
[3] D. Bloor and R.R. Chance, *Polydiacetylenes: Synthesis, Structure, and Electronic Properties* (Nijhoff, Dordrecht, 1985).
[4] R.A. Nallicheri and M.F. Rubner, Macromolecules 24 (1991) 517.
[5] R.W. Carpick, D.Y. Sasaki and A.R. Burns, Langmuir 16 (2000) 1270.
[6] R.W. Carpick, T.M. Mayer, D.Y. Sasaki and A.R. Burns, Langmuir 16 (2000) 4639.
[7] D.Y. Sasaki, R.W. Carpick and A.R. Burns, J. Colloid Interface Sci. (2000), in press.
[8] D.H. Charych, J.O. Nagy, W. Spevak and M.D. Bednarski, Science 261 (1993) 585.
[9] S. Okada, S. Peng, W. Spevak and D. Charych, Acc. Chem. Res. 31 (1998) 229.
[10] U. Jonas, K. Shah, S. Norvez and D.H. Charych, J. Am. Chem. Soc. 121 (1999) 4580.
[11] M.D. Mowery and C.E. Evans, J. Phys. Chem. B 101 (1997) 8513.
[12] Z.G. Soos, D.S. Galvao and S. Etemad, Adv. Mater. 6 (1994) 280.
[13] F. Garnier, Acc. Chem. Res. 32 (1999) 209.
[14] J.-L. Bredas, J. Cornil, D. Beljohnne, D.A. Dos Santos and Z. Shuai, Acc. Chem. Res. 32 (1999) 267.
[15] R.W. Carpick, D.Y. Sasaki and A.R. Burns, Tribol. Lett. 7 (1999) 79.
[16] H. Eckhardt, D.S. Boudreaux and R.R. Chance, J. Chem. Phys. 85 (1986) 4116.
[17] K.S. Schweizer, J. Chem. Phys. 85 (1985) 1156.
[18] K.S. Schweizer, J. Chem. Phys. 85 (1985) 1176.
[19] V. Dobrosavljevic and R.M. Stratt, Phys. Rev. B 35 (1987) 2781.
[20] G. Rossi, R.R. Chance and R. Silbey, J. Chem. Phys. 90 (1989) 7594.
[21] M.D. Mowery, S. Kopta, D.F. Ogletree, M. Salmeron and C.E. Evans, Langmuir 15 (1999) 5118.
[22] A. Lio, A. Reichert, D.J. Ahn, J.O. Nagy, M. Salmeron and D.H. Charych, Langmuir 13 (1997) 6524.
[23] R.F. Fischetti, M. Filipkowski, A.F. Garito and J.K. Blasie, Phys. Rev. B 37 (1988) 4714.
[24] J.N. Israelachvili, *Intermolecular and Surface Forces* (Academic Press, London, 1992).